catalysts

MDPI

Supplementary Materials

The Application of Copper-Gold Catalysts in the Selective Oxidation of Glycerol at Acid and Basic Conditions

Piotr Kaminski

Adam Mickiewicz University, Faculty of Chemistry, Department of Rare Earths,
ul. Uniwersytetu Poznańskiego 8, 61-614, Poznań, Poland; piotr.kaminski@amu.edu.pl
Correspondence: piotr.kaminski@amu.edu.pl; phone number: +48-61-829-1832

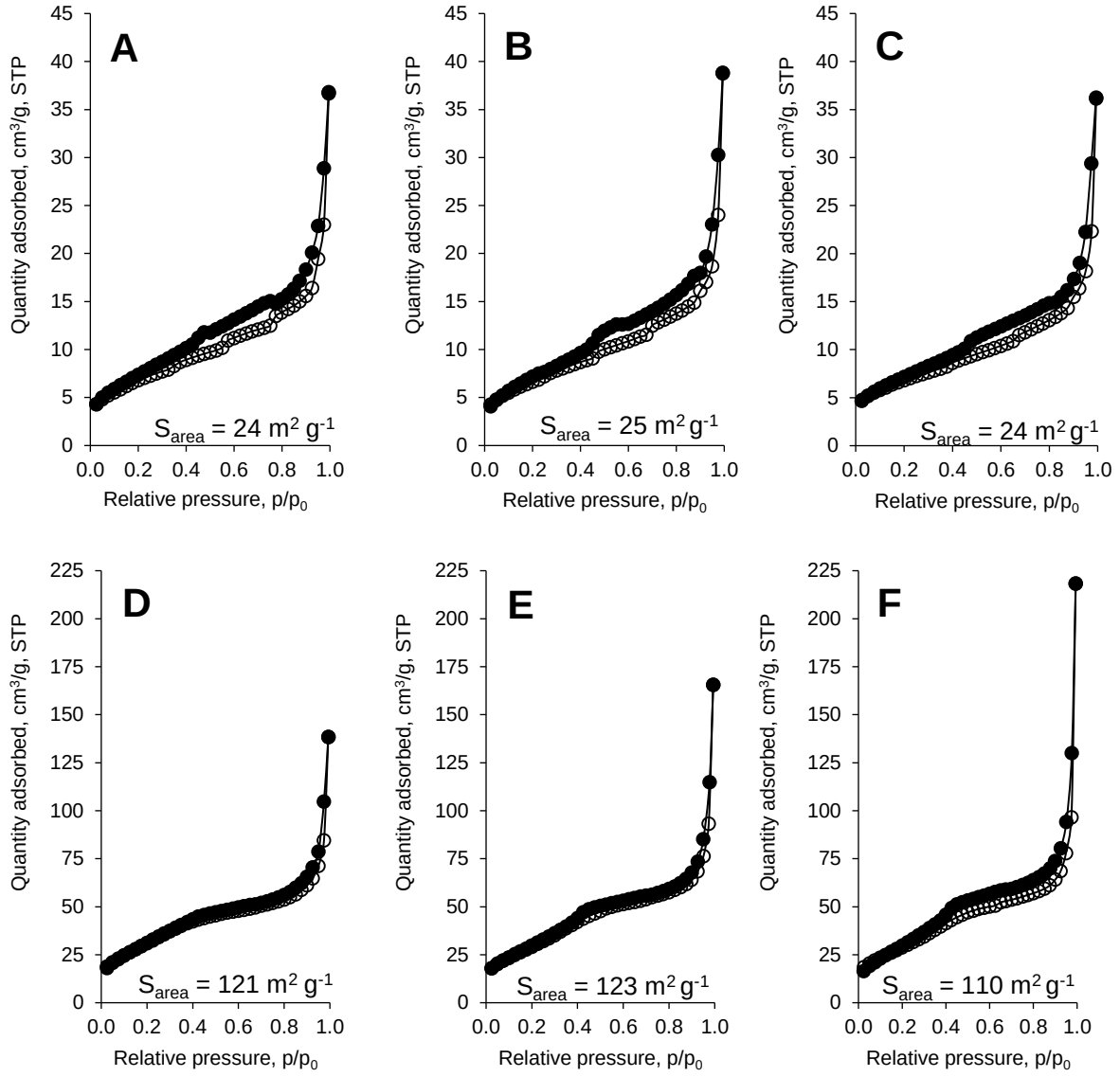

Fig. S1. Isotherms of adsorption and desorption of nitrogen at 77 K performed for: (A) CeO_2; (B) Au/CeO_2; (C) $CuAu/CeO_2$; (D) ZrO_2; (E) Au/ZrO_2 and (F) $CuAu/ZrO_2$, before their application as catalysts in glycerol oxidation.

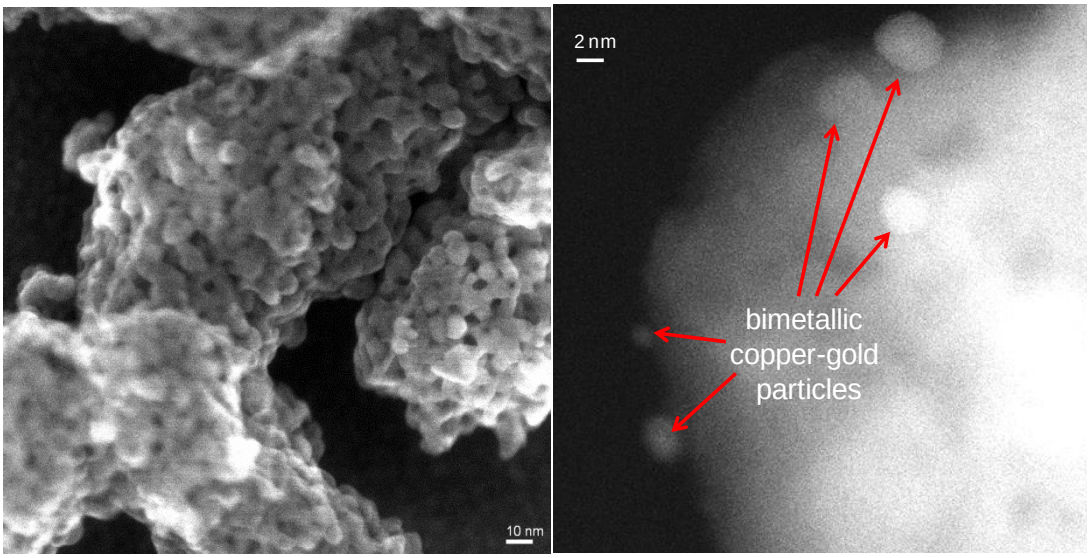

Fig. S2. The SEM (left side) and TEM (right side) images recorded for CuAu/ZrO_2 before its application in glycerol oxidation.

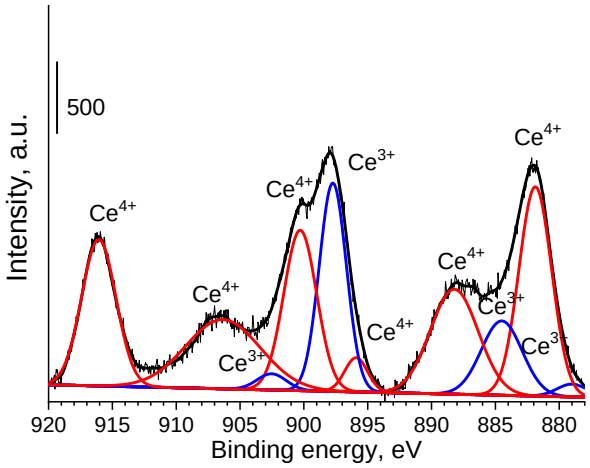

Fig. S3. The XP spectra of 3d Ce species region recorded for $CuAu/CeO_2$ after its application as catalyst in glycerol oxidation in the presence of hydrogen peroxide.

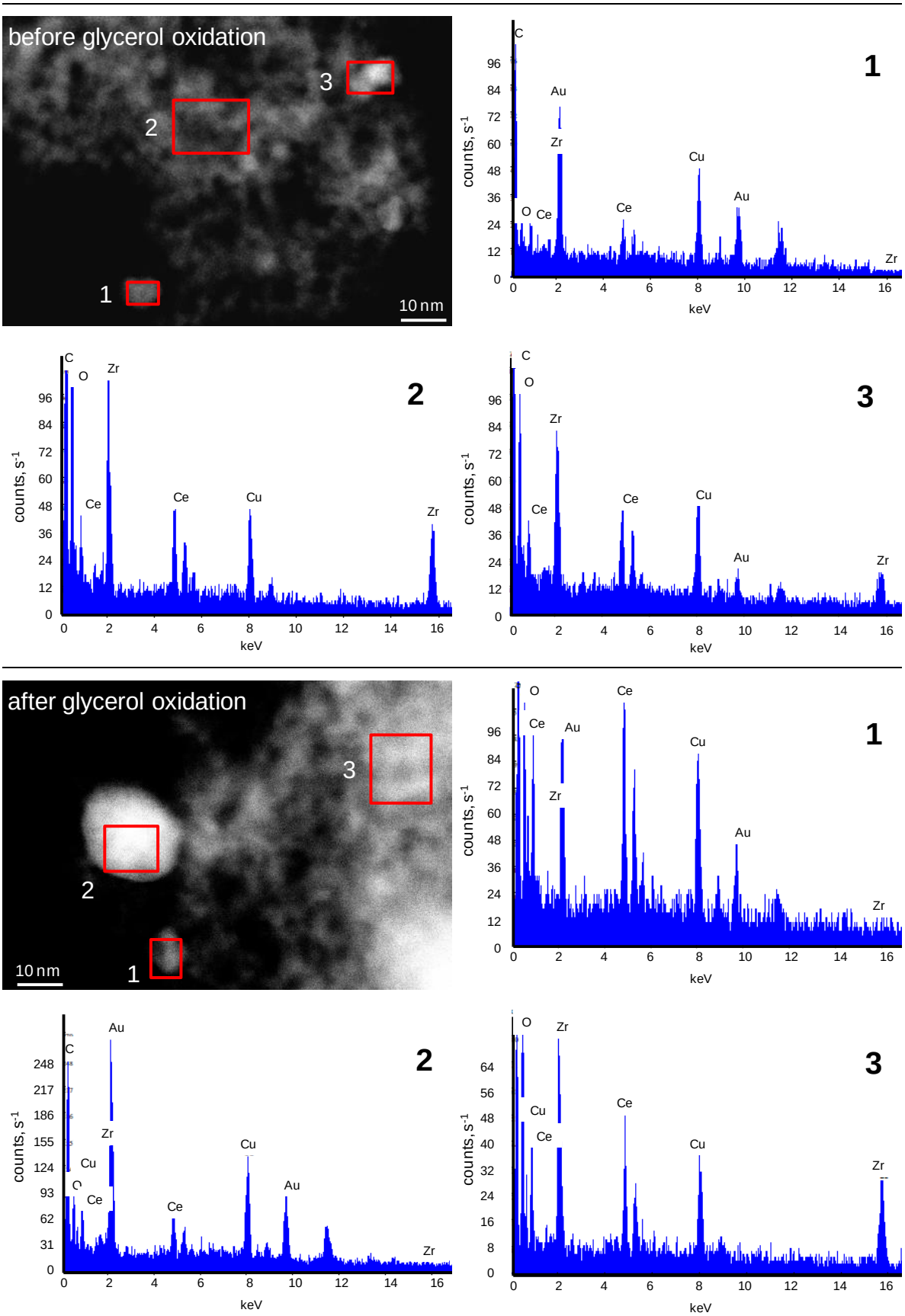

Fig. S4. STEM images and EDX spectra recorded for CuAu/CeZrO$_x$ before and after its application as catalyst in glycerol oxidation.

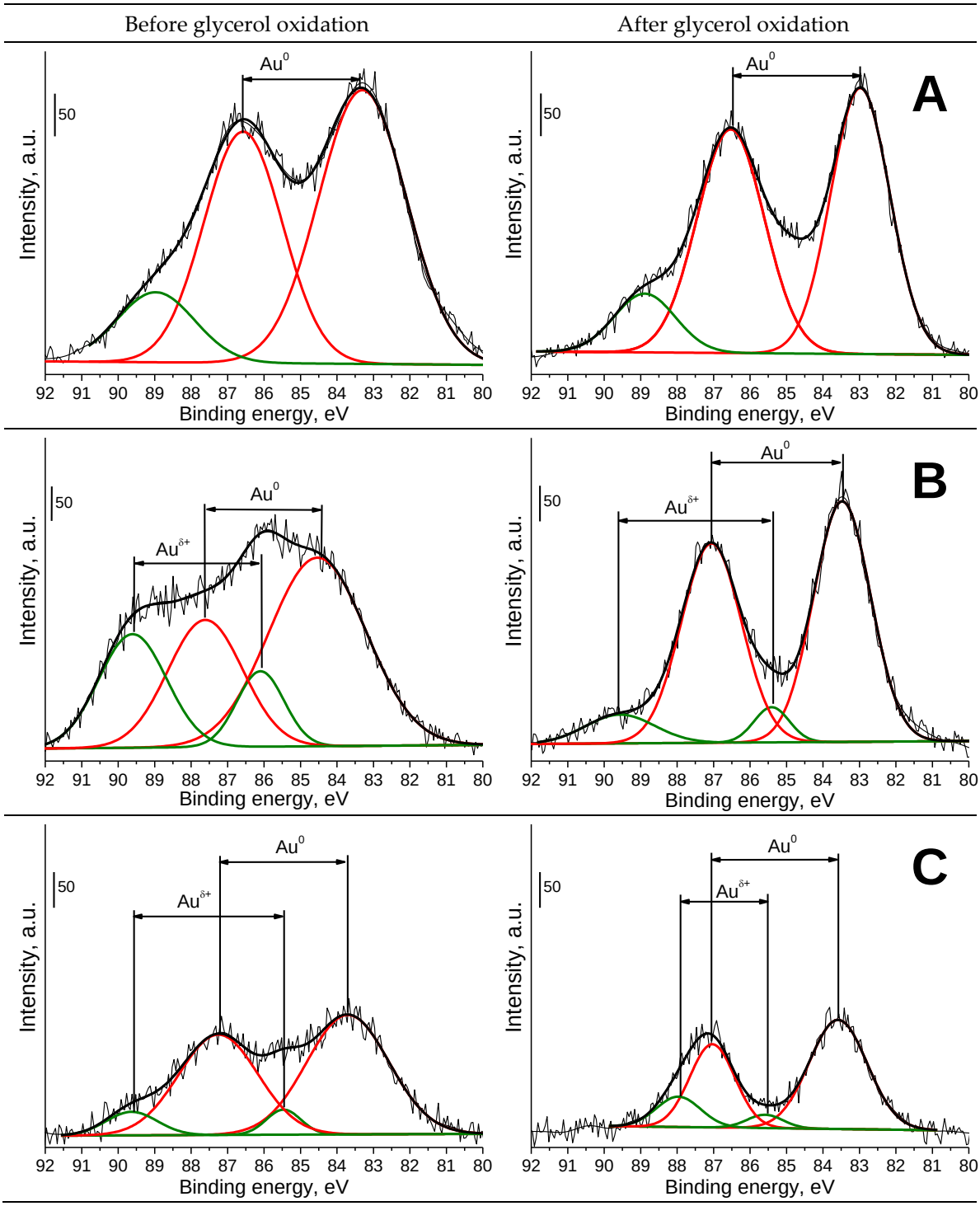

Fig. S5. XP spectra of 4f Au species region recorded for: (A) Au/CeO_2; (B) Au/$CeZrO_x$ and (C) Au/ZrO_2 before and after their application as catalysts in glycerol oxidation.

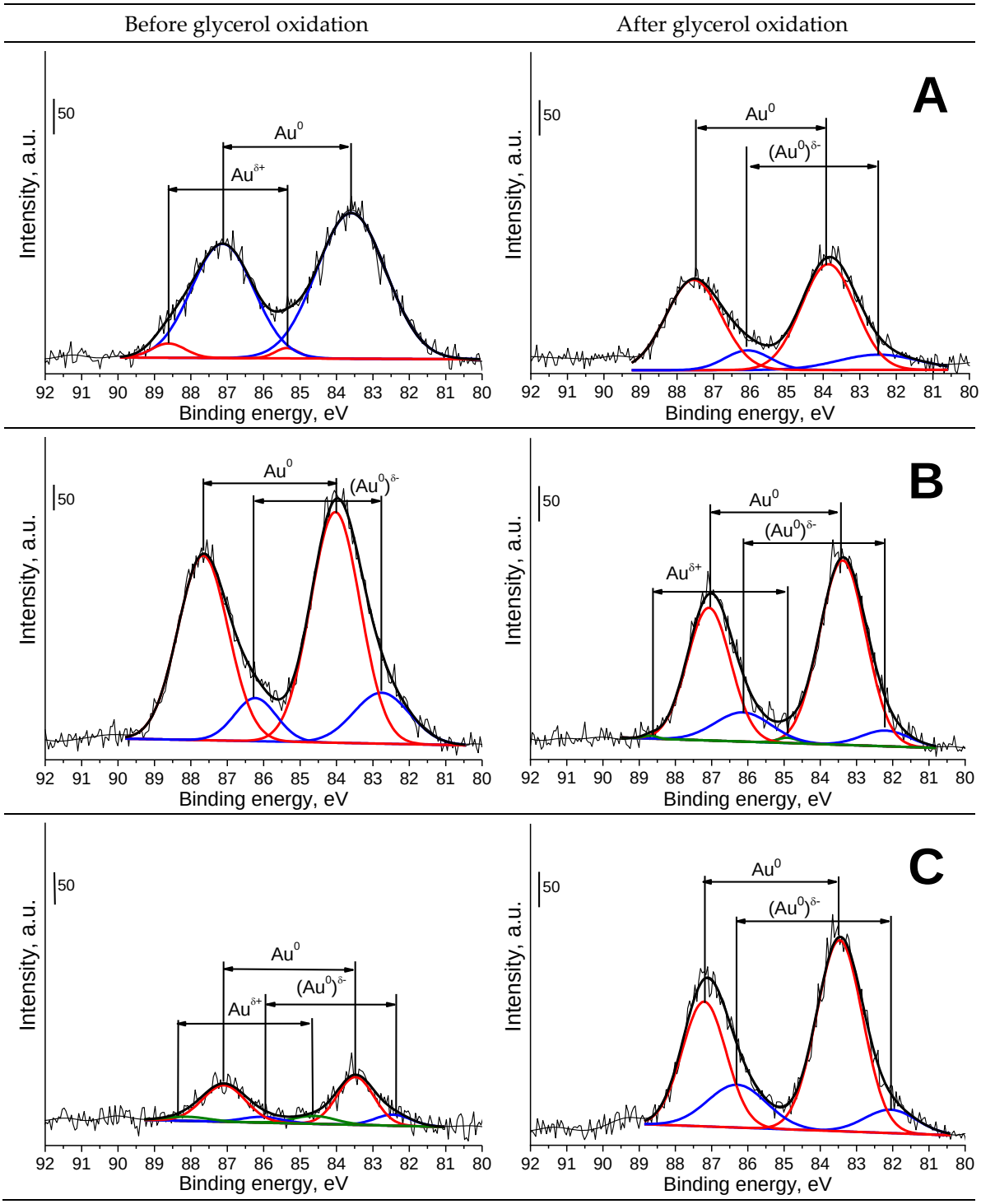

Fig. S6. XPS spectra of 4f Au species region recorded for: (A) CuAu/CeO_2; (B) CuAu/$CeZrO_x$ and (C) CuAu/ZrO_2 before and after their application as catalysts in glycerol oxidation.

The chemical composition of supports affected the distribution of gold species. In the case of catalysts before their application in glycerol oxidation, the highest gold content on the external surface was noted in the catalysts based on pure ceria and mixed cerium-zirconium oxide (Table S1).

The XP spectra performed for the catalysts with gold species showed the presence of two bands which can be due to the spin-orbit components Au $4f_{7/2}$ and Au $4f_{5/2}$ [1-5], which can be attributed to two different gold species (Figures S5 and S6), corresponding to $(Au^0)^{\delta-}$, Au^0 and/or $Au^{\delta+}$ species, where δ means +1 and/or +3. According to literature [6,7], the binding energy (BE) of Au $4f_{7/2}$ for bulk metallic gold Au^0 is 83.0-84.4 eV, for Au^+ – 84.5-85.0 eV and for Au^{3+} – 85.0-86.5 eV. It is very difficult to distinguish Au^+ and Au^{3+} species because the presented above limits of BE ranges are not rigid and this is the reason why in this work all cationic gold species are described as $Au^{\delta+}$.

In the case of monometallic gold catalysts, the BE due to metallic gold (Au^0) changed from 83.0 to 84.5 eV (Fig. S5). In the case of Au/CeO_2 catalysts, BE was at 83.2 and 83.0 eV, before and after glycerol oxidation, respectively (Table S2), and these values are lower than in the bulk metallic gold (84.0 eV) [8]. It has been reported [3,9,10] that gold species characterised by BE in the range 82-83 eV can be due to the partial negative charge on the external surface of metallic gold particles. The XP spectra Au 4f species performed for copper-gold catalysts were characterised by two bands (excepting CuAu/ZrO_2 before glycerol oxidation and CuAu/$CeZrO_x$ after glycerol oxidation) (Fig. S6). In CuAu/CeO_2 catalyst, the gold species can be due to Au $4f_{7/2}$ species at 83.6 and 85.4 eV (before glycerol oxidation) and at 82.5 and 83.9 eV (after glycerol oxidation) and these values of BE can be attributed to Au^0 and $Au^{\delta+}$ (before glycerol oxidation) and $(Au^0)^{\delta-}$ and Au^0 (after glycerol oxidation), respectively. On the mixed cerium-zirconium oxide modified with gold and copper (CuAu/$CeZrO_x$), two bands were observed at 82.3 and 83.6 eV before glycerol oxidation and three bands at 82.2, 83.4 and 84.9 eV after glycerol oxidation. These bands can be due to the metallic gold particles with the partial negative charge on the external surface of metallic gold particles ($(Au^0)^{\delta-}$) and metallic gold (Au^0) (before glycerol oxidation) and to $(Au^0)^{\delta-}$, Au^0 and $Au^{\delta+}$ (after glycerol oxidation), respectively. In the case of CuAu/ZrO_2 catalyst, gold species gave the bands at 82.4, 83.5 and 84.6 eV (before glycerol oxidation) and at 82.1 and 83.5 eV (after glycerol oxidation), respectively. The lower BE of metallic gold species in the case of bimetallic catalysts than in monometallic catalysts can be explained by the appearance of the smaller gold particles loading on the surface of catalysts [1,11]. The presence of very small metallic gold particles in the bimetallic catalysts was confirmed by the STEM-EDX spectroscopy (Fig. S4).

An according to the literature data [12,13], the BE of Cu 2p species could be assigned to Cu^0, Cu^+ and Cu^{2+} in the range of 930.0-932.0, 932.0-933.0 and 933.0-935.5 eV, respectively. The bimetallic copper-gold catalysts before and after their using in glycerol oxidation were the samples in which the copper was in the reduced form – Cu^+ cation (excluding CuAu/$CeZrO_2$ after its using in glycerol oxidation). It is interesting that in all bimetallic catalysts after their using in the glycerol oxidation, in the case of copper (species Cu^+), the first part was reduced to metallic copper (Cu^0) and the second part oxidized to cationic copper (Cu^{2+}) and the growth of zirconium content in the support led to more significant the decrease of the distribution of Cu^+ species. The lower distribution of Cu^+ species in the bimetallic catalysts was accompanied by the growth of the distribution of gold species as like metallic gold particles with the partial negative charge on the external surface ($(Au^0)^{\delta-}$). It can be explained by the parallel partial reduction of metallic gold (Au^0) to $(Au^0)^{\delta-}$ and the disproportion reaction of cationic copper (Cu^+) to metallic copper (Cu^0) and cationic copper (Cu^{2+}) during the oxidation of glycerol in the liquid phase.

Table S1. The composition of catalysts (estimated using XPS) before and after their application in glycerol oxidation at 333 K for 5 h at 1200 rpm at basic conditions.

Catalyst	Content of metal species, wt %		Au:Cu molar ratio
	Au, before/after	Cu, before/after	before/after
Au/CeO_2	10.0/6.8	–/–	–/–
$Au/CeZrO_x$	9.1/5.3	–/–	–/–
Au/ZrO_2	2.6/2.4	–/–	–/–
$CuAu/CeO_2$	8.2/3.0	2.7/1.5	0.99/0.64
$CuAu/CeZrO_x$	11.4/3.8	2.1/1.7	1.78/0.74
$CuAu/ZrO_2$	0.9/6.4	1.8/2.4	0.16/0.85

Table S2. The BE of gold and copper species in the selected catalysts before and after their application in glycerol oxidation.

Catalyst	Binding energy (BE), eV					
	Au $4f_{7/2}$ species			Cu $2p_{3/2}$ Species		
	$(Au^0)^{\delta-}$	Au^0	$Au^{\delta+}$	Cu^0	Cu^+	Cu^{2+}
Au/CeO_2 before	-	83.2	-	-	-	-
Au/CeO_2 after	-	83.0	-	-	-	-
$Au/CeZrO_x$ before	-	84.5	86.1	-	-	-
$Au/CeZrO_x$ after	-	83.5	85.4	-	-	-
Au/ZrO_2 before	-	83.7	85.5	-	-	-
Au/ZrO_2 after	-	83.6	85.6	-	-	-
$CuAu/CeO_2$ before	-	83.6	85.4	-	932.0	934.9
$CuAu/CeO_2$ after	82.5	83.9	-	930.6	932.5	934.5
$CuAu/CeZrO_x$ before	82.3	83.6	-	-	933.3	935.0
$CuAu/CeZrO_x$ after	82.2	83.4	84.9	930.2	932.8	935.0
$CuAu/ZrO_2$ before	82.4	83.5	84.6	-	932.2	934.3
$CuAu/ZrO_2$ after	82.1	83.5	-	931.0	932.6	934.2

References

1. Dimitratos, N.; Villa, A.; Bianchi, C.L.; Prati, L.; Makkee, M. Gold on titania: Effect of preparation method in the liquid phase oxidation. *Appl. Catal. A: Gen.* **2006**, *311*, 185-192. DOI: https://doi.org/10.1016/j.apcata.2006.06.026 (accessed on 29.12.2020)
2. Chang, F.-W.; Yu, H.-Y.; Roselin, L.S.; Yang, H.-C.; Ou, T.-C. Hydrogen production by partial oxidation of methanol over gold catalysts supported on TiO_2-MO_x (M = Fe, Co, Zn) composite oxides. *Appl. Catal. A: Gen.* **2006**, *302*, 157-167. DOI: https://doi.org/10.1016/j.apcata.2005.12.028 (accessed on 29.12.2020)
3. Bogdanchikova, N.; Pestryakov, A.; Tuzovskaya, I.; Zepeda, T.A.; Farias, M.H.; Tiznado, H.; Martynyuk, O. Effect of redox treatments on activation and deactivation of gold nanospecies supported on mesoporous silica in CO oxidation. *Fuel* **2013**, *110*, 40-47. DOI: https://doi.org/10.1016/j.fuel.2012.09.064 (accessed on 29.12.2020)

4. Hua, J.; Wie, K.; Zheng, Q.; Lin, Z. Influence of calcination temperature on the structure and catalytic performance of Au/iron oxide catalysts for water–gas shift reaction. *Appl. Catal. A: Gen.* **2004**, *259*, 121-130. DOI: https://doi.org/10.1016/j.apcata.2003.09.028 (accessed on 29.12.2020)
5. Zwijnenburg, A.; Goosens, A.; Sloof, W.G.; Graje, M.W.J.; Kraan, A.M.; Jongth, L.J.; Makee, M.; Moulijn, J.A. XPS and Mössbauer Characterization of Au/TiO_2 Propene Epoxidation Catalysts. *J. Phys. Chem. B* **2002**, *106*, 9853-9862. DOI: https://doi.org/10.1021/jp014723w (accessed on 29.12.2020)
6. Albonetti, S.; Pasini, T.; Lolli, A.; Blosi, M.; Piccinini, M.; Dimitratos, N.; Lopez-Sanchez, J.A.; Morgan, D.J.; Carley, A.F.; Hutchings, G.J.; Cavani, F. Selective oxidation of 5-hydroxymethyl-2-furfural over TiO_2-supported gold–copper catalysts prepared from preformed nanoparticles: Effect of Au/Cu ratio. *Catal. Today* **2012**, *195*, 120-126. DOI: https://doi.org/10.1016/j.cattod.2012.05.039 (accessed on 29.12.2020)
7. Smolentseva, E.; Simakov, A.; Beloshapkin, S.; Estrada, M.; Vargas, E.; Sobolev, V.; Kenzhin, R.; Fuentes, S. Gold catalysts supported on nanostructured Ce–Al–O mixed oxides prepared by organic sol–gel. *Appl. Catal. B: Environ.* **2012**, *115-116*, 117-128. DOI: https://doi.org/10.1016/j.apcatb.2011.12.010 (accessed on 29.12.2020)
8. Moulder, J.F.; Stickle, W.F.; Sobol, P.E.; Bomben, K.D. Handbook of X-ray Photoelectron Spectroscopy. Publisher: Perkin-Elmer Corporation, Physical Electronics Division, USA, Eden Prairie, 1992; ISBN: 096481241X and 9780964812413.
9. Xu, J.; White, T.; Li, P.; He, C.; Yu, J.; Yuan, W.; Han, Y-.F. Biphasic Pd−Au Alloy Catalyst for Low-Temperature CO Oxidation. *J. Am. Chem. Soc.* **2010**, *132*, 10398-10406. DOI: https://doi.org/10.1021/ja102617r (accessed on 29.12.2020)
10. Wang, A.-Q.; Liu, J.-H.; Lin, S.-D.; Lin, T.-S.; Mou, C.-Y. A novel efficient Au–Ag alloy catalyst system: preparation, activity, and characterization. *J. Catal.* **2005**, *233*, 186-197. DOI: https://doi.org/10.1016/j.jcat.2005.04.028 (accessed on 29.12.2020)
11. Tuzovskaya, I.; Bogdanchikova, N.; Simakov, A.; Gurin, V.; Pestryakov, A.; Avalos, M.; Farias, M.H. Structure and electronic states of gold species in mordenites. *Chem. Phys.* **2007**, *338*, 23–32. DOI: https://doi.org/10.1016/j.chemphys.2007.07.026 (accessed on 29.12.2020)
12. Llorca, J.; M. Domínguez, J.; Ledesma, C.; Chimentão, R.J.; Medina, F.; Sueiras, J.; Angurell, I.; Seco, M.; Rossell, O. Propene epoxidation over TiO_2-supported Au–Cu alloy catalysts prepared from thiol-capped nanoparticles. *J. Catal.* **2008**, *258*, 187-198. DOI: https://doi.org/10.1016/j.jcat.2008.06.010 (accessed on 29.12.2020)
13. Gupta, A.; Waghmare, U.V.; Hegde, M.S. Correlation of Oxygen Storage Capacity and Structural Distortion in Transition-Metal-, Noble-Metal-, and Rare-Earth-Ion-Substituted CeO_2 from First Principles Calculation. *Chem. Mater.* **2010**, *22*, 5184-5198. DOI: https://doi.org/10.1021/cm101145d (accessed on 29.12.2020)